Supplementary Information

NIR optical carbon dioxide gas sensor based on simple azaBODIPY pH indicators

M.D. Fernández-Ramos*[a,d], M.L. Aguayo-López[a], E. de los Reyes-Berbel[b], F. Santoyo González[b,c,d] and L.F. Capitán-Vallvey[a,d]

[a]ECsens. Department of Analytical Chemistry, University of Granada, Granada 18071 (Spain). [b]Department of Organic Chemistry, Faculty of Sciences. [c] Institute of Biotechnology, University of Granada, E-18071 (Spain). [d] Unit of Excellence in Chemistry applied to biomedicine and the environment of the University of Granada.

*e-mail: mdframos@ugr.es

Table of Contents

1. X-Ray Powder Diffraction analysis of GAB.

The microcrystalline GAB synthetized was gently ground in an agate mortar and then deposited with care in the hollow of an aluminium holder equipped with a zero background plate. Diffraction data (Cuα, $\lambda = 1.5418$ Å) were collected on a θ:θ Bruker AXS D8 vertical scan diffractometer equipped with primary and secondary Soller slits, a secondary beam curved graphite monochromator. The generator was operated at 40 kV and 40 mA. A long scan was performed with $5 < 2\theta < 35°$ with $t = 1$ s and $\Delta 2\theta = 0.02°$. Figure 1 show published (a) [1] and experimental (b) diffraction patterns. After analysing the spectra, we can conclude that these compounds are isostructural materials. LeBail refinement was performed and found similar values of unit cell for *R32* Space group (a = 9.348 Å, c = 7.312 Å) with a sample displacement of 0.29 mm.

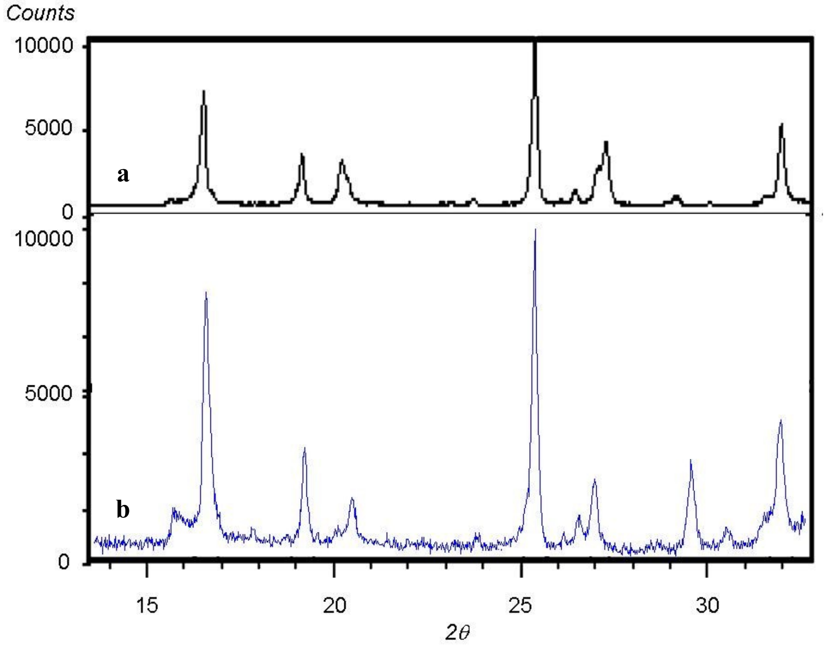

Figure S1. GAB X-ray difference diffraction patterns: published (black) and experimental (blue)

2. Microcrystalline GAB particle size

The size of the microcrystals was calculated as the mean of 10 measurements using a fluorescence microscope, Olympus DP72 Microscope Digital Camera with a filter TRIC being 0.5 µm.

Table S1. Particle size of microcrystalline GAB.

Particle size (µm)										SRD (%)
0.64	0.51	0.52	0.52	0.50	0.64	0.52	0.50	0.51	0.52	10

3. Characterization spectra of BODIPY

aBI:

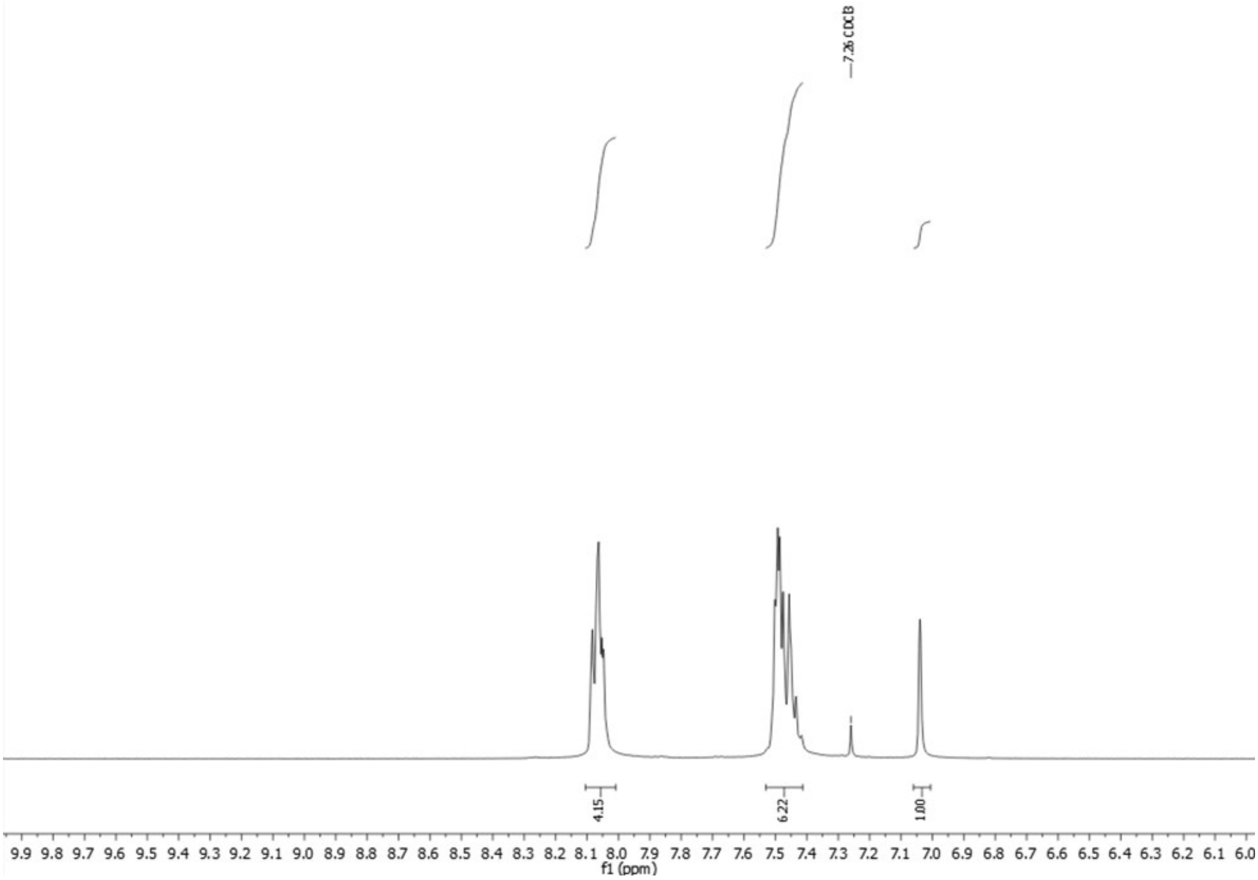

Figure S2. 1H NMR (400 MHz, Chloroform-d) δ 8.06 (tq, J = 5.9, 3.4, 2.7 Hz, 8H), 7.55 – 7.40 (m, 12H), 7.07 – 7.01 (m, 2H)

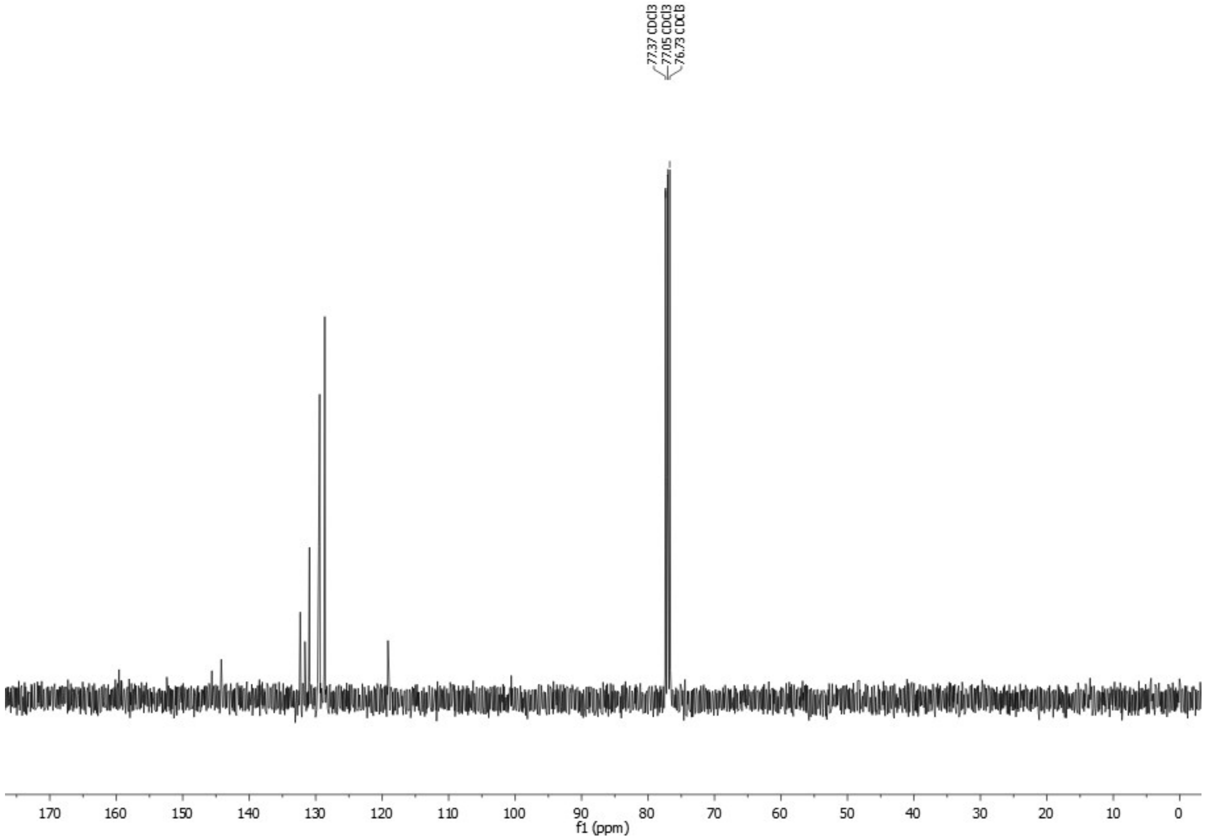

Figure S3. 13C NMR (101 MHz, CDCl3) δ 159.59, 144.21, 132.33, 131.62, 130.93, 129.63, 129.59, 129.54, 129.41, 128.66, 128.63, 119.13,

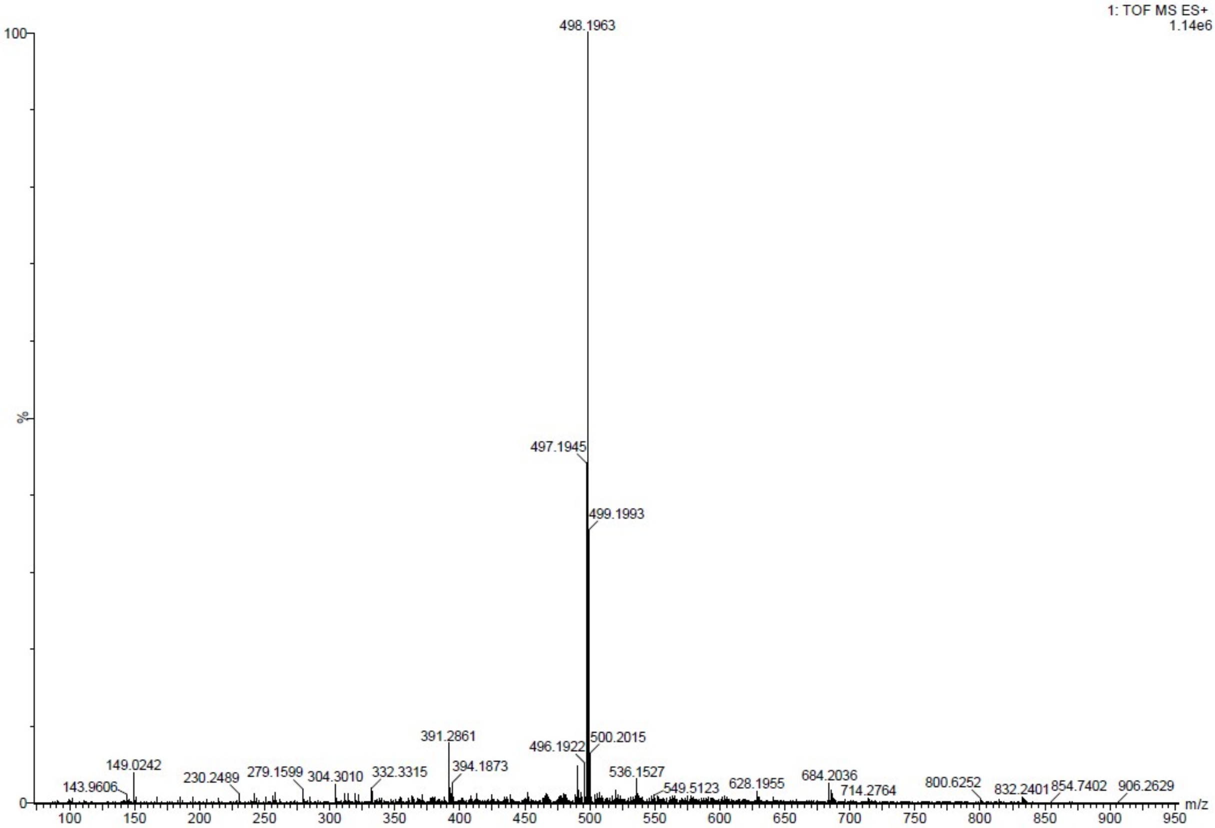

Figure S4. ESI-MS (HDMS Q-TOF) m/z calculated for ($C_{32}H_{23}BF_2N_3$) $[M+H]^+$ 498.1953, found 498.1963.

aBII:

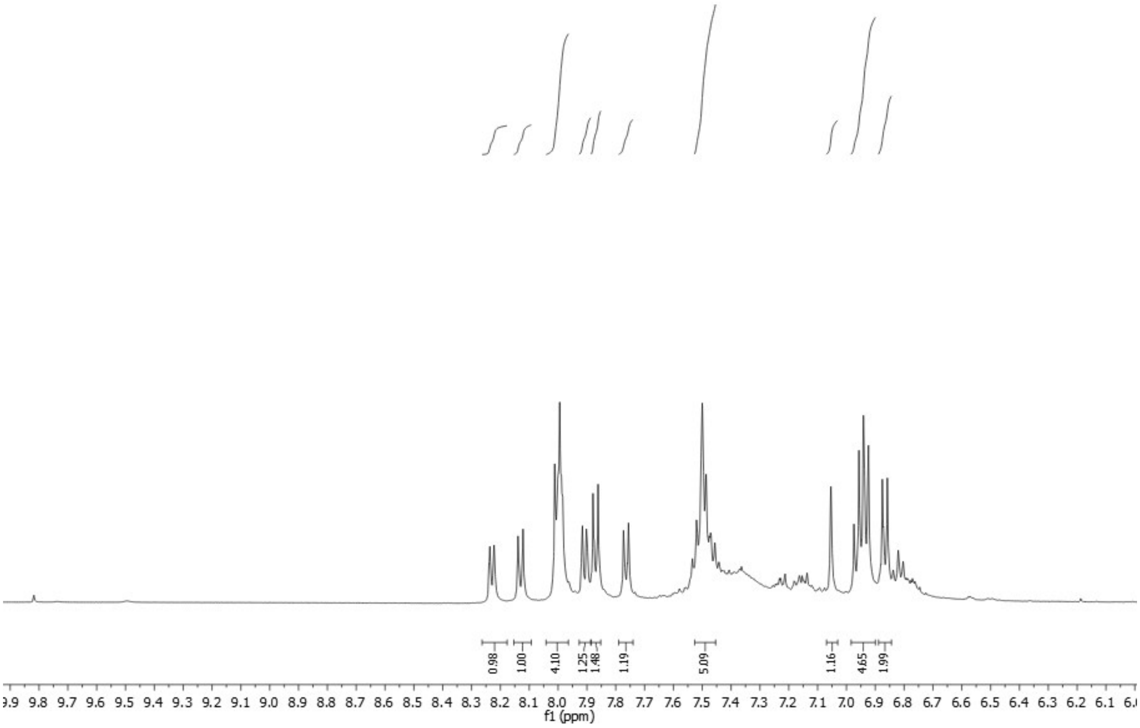

Figure S5. ^{1}H NMR (500 MHz, Acetonitrile-d_3) δ 8.26 – 8.20 (m, 1H), 8.15 – 8.09 (m, 1H), 8.00 (ddt, J = 10.3, 5.6, 3.2 Hz, 4H), 7.93 – 7.88 (m, 1H), 7.88 – 7.84 (m, 1H), 7.79 – 7.73 (m, 1H), 7.50 (td, J = 4.6, 2.3 Hz, 5H), 7.05 (d, J = 1.4 Hz, 1H), 6.98 – 6.90 (m, 5H), 6.90 – 6.84 (m, 2H).

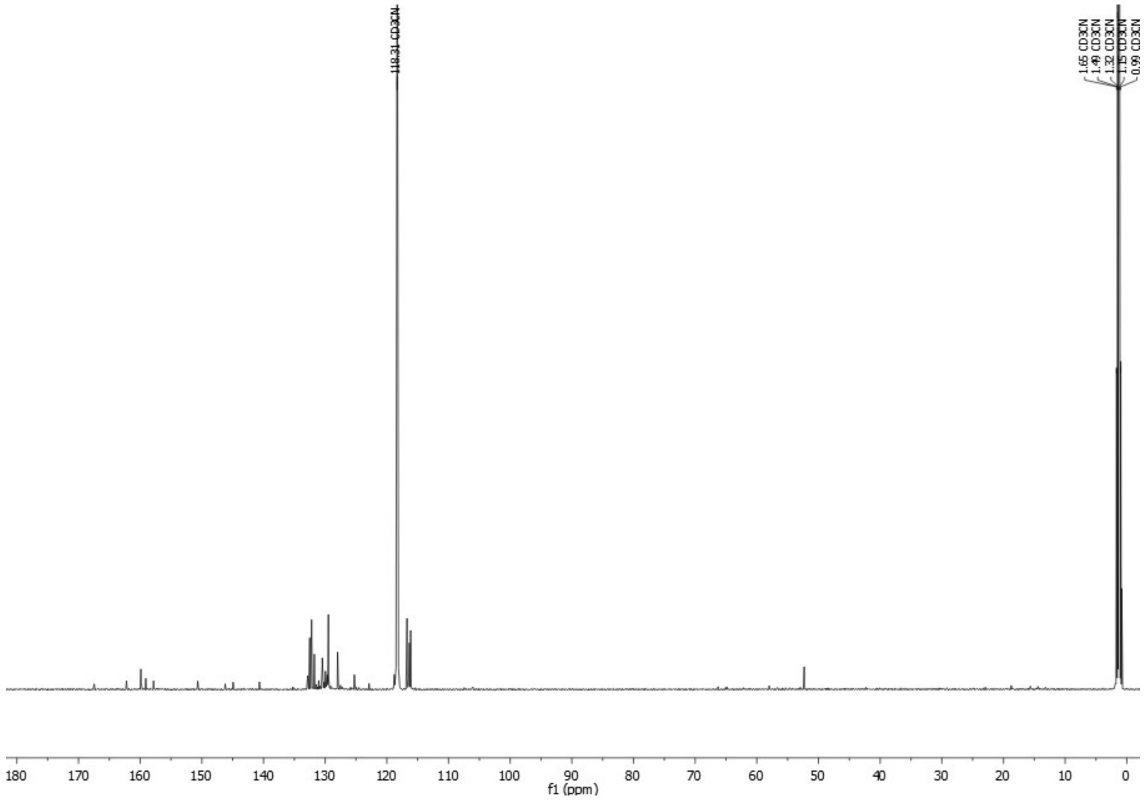

Figure S6. ^{13}C NMR (126 MHz, CD_3CN) δ 162.20, 159.88, 159.08, 157.83, 132.81, 132.51, 132.20, 131.75, 131.04, 130.49, 130.46, 130.43, 129.96, 129.63, 129.51, 129.47, 127.98, 125.26, 116.78, 116.72, 116.43, 116.33, 116.30, 116.13.

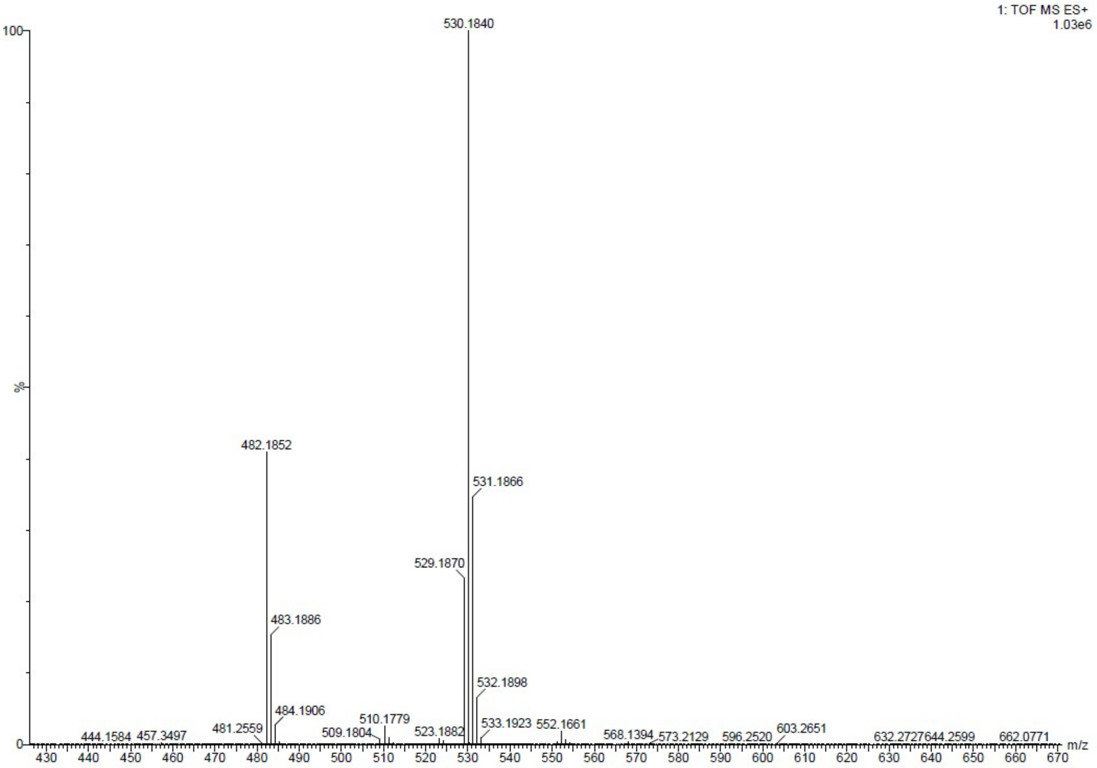

Figure S7. ESI-MS (HDMS Q-TOF) m/z calculated for ($C_{32}H_{23}BF_2N_3O_2$) $[M+H]^+$ 530.1851, found 530.1859.

The NMR experiments were performed on a 400 MHz high definition nuclear magnetic resonance BRUKER Nanobay Avance III HD spectrometer.

The ESI-MS experiments were performed on a liquid chromatography system hybrid mass spectrometer SYNAPT G2 HDMS Q-TOF model (Waters, Milford, USA)

4. Mass spectra of BODIPY

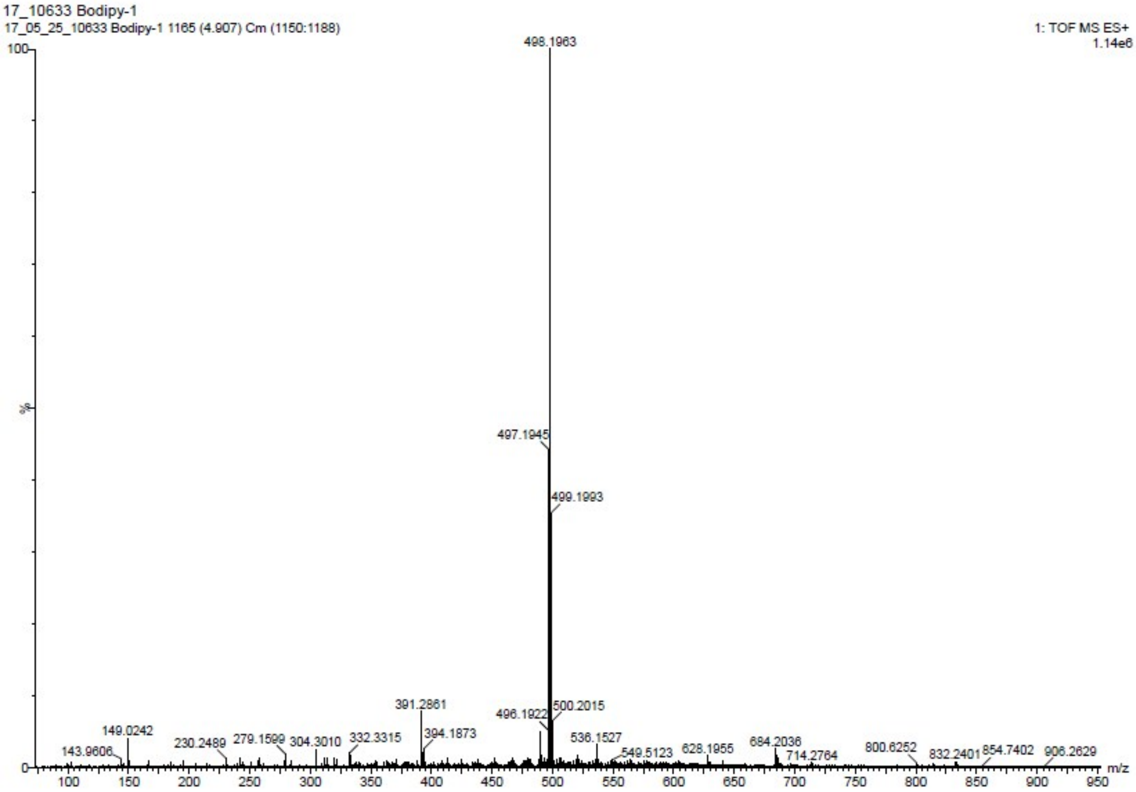

Figure S8. Mass spectrum of azaBODIPY I.

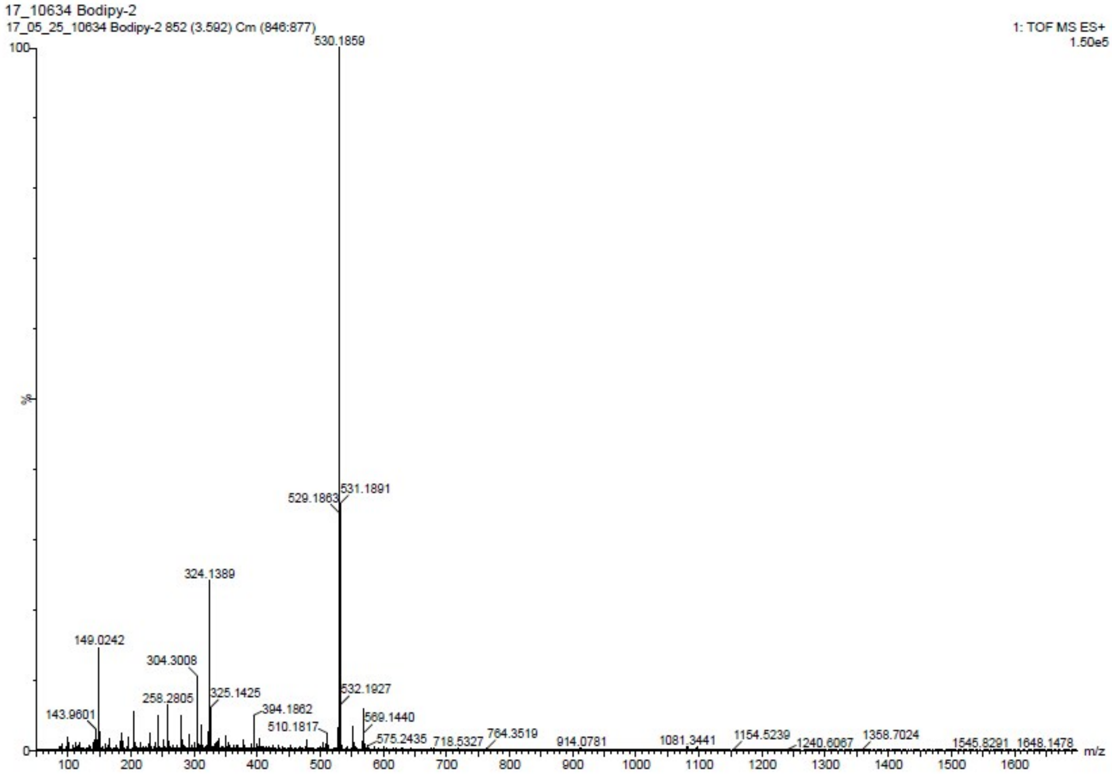

Figure S9. Mass spectrum of azaBODIPY II

Table S2. AzaBODIPY molecular masses calculated and obtained by mass spectrometry measurement.

Product	Structure	Empirical formula + H^{+*}	Calculate molecular mass	Obtained molecular mass
azaBODIPY I	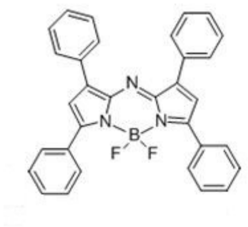	$C_{32}H_{23}BF_2N_3$	498.1953	498.1963
azaBODIPY II	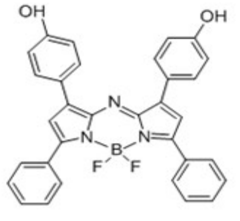	$C_{32}H_{23}BF_2N_3O_2$	530.1851	530.1859

*The two azaBODIPYs synthesized are in protonated form, and in all cases three cases the product obtained had one hydrogen atom more than appears in the original molecular structure.

5. Physical and chemical properties of azaBODIPY.

In order to determine the molar absorptivity, stock solutions of the each BODIPY were prepared by weighing the powder on a 5-digit analytical balance in a glass vial and solving in toluene for azaBODIPY I (final concentration $4.04 \cdot 10^{-2}$ mM), ethanol for azaBODIPY II ($2.95 \cdot 10^{-2}$ mM). Working solutions were prepared by further dilution of the stock solutions with the same solvent with concentrations ranging from 0.2 to 8 μM and 20 to 80 μM for azaBODIPY I and II respectively. The absorbance at the wavelength of maximum absorbance was plotted vs the final dye concentration to obtain the calibration graph. Finally, the corresponding regression equation was derived according to Lambert-Beer law.

Relative fluorescence quantum yield was estimated according to equation 1[2].

$$\emptyset_{FV} = \emptyset_R \frac{m_{FV}}{m_R} \left(\frac{\mu_{FV}}{\mu_R} \right)^2 \quad \text{(eq.1)}$$

Where ϕ_{FV} is the quantum yield of the fluorochrome problem; ϕ_R is the quantum yield of the fluorochrome standard; μ_{FV} is the refractive index of the solvent used for the fluorochrome problem; μ_R is the refractive index of the solvent used for the fluorochrome standard; m_{FV} and m_R are the respective slope of the integrated fluorescence intensity vs absorbance for problem and standard.

In order to determination of decay time a fit via monoexponential decay model was used for both azaBodipys was made (Figure S10).

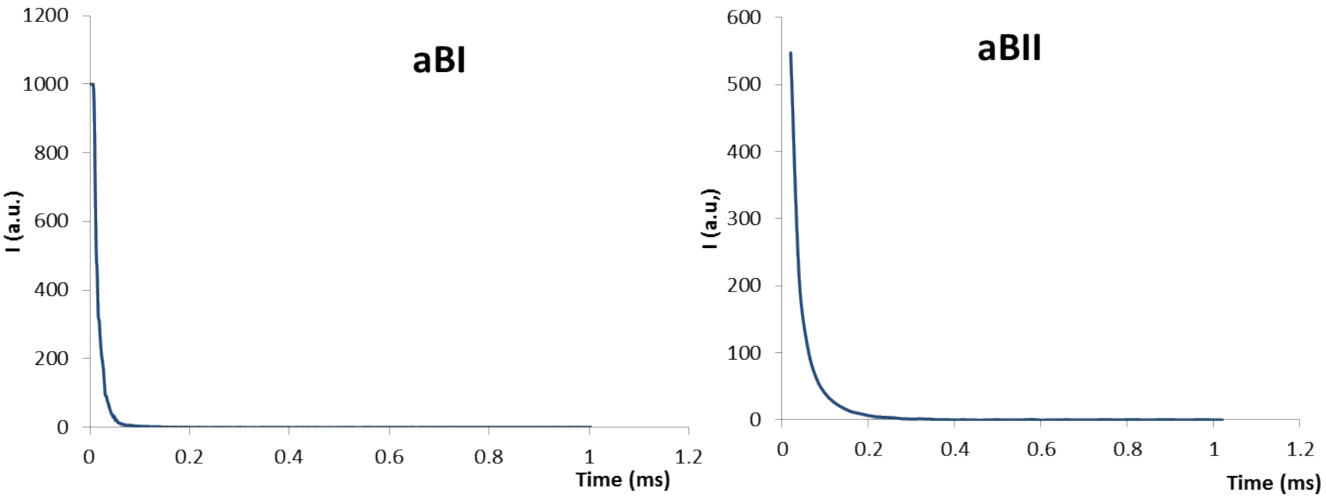

Figure S10. Decay times fit vía monoexponential decay model for aBI and aBII.

6. Acid-base characteristics of azaBODIPY.

The pKa values of azaBODIPY were determined by modifying the pH of solutions: a) For azaBODIPY I in 3:1 v/v dimethylsulfoxide:water from 6.80 to 9.30 through successive addition of $1\cdot10^{-4}$ M NaOH solution (Figure S11); b) For azaBODIPY II in 1:1 v/v ethanol:water from 5.95 to 10.30 by addition of $1\cdot10^{-3}$ M NaOH solution (Figure S12)

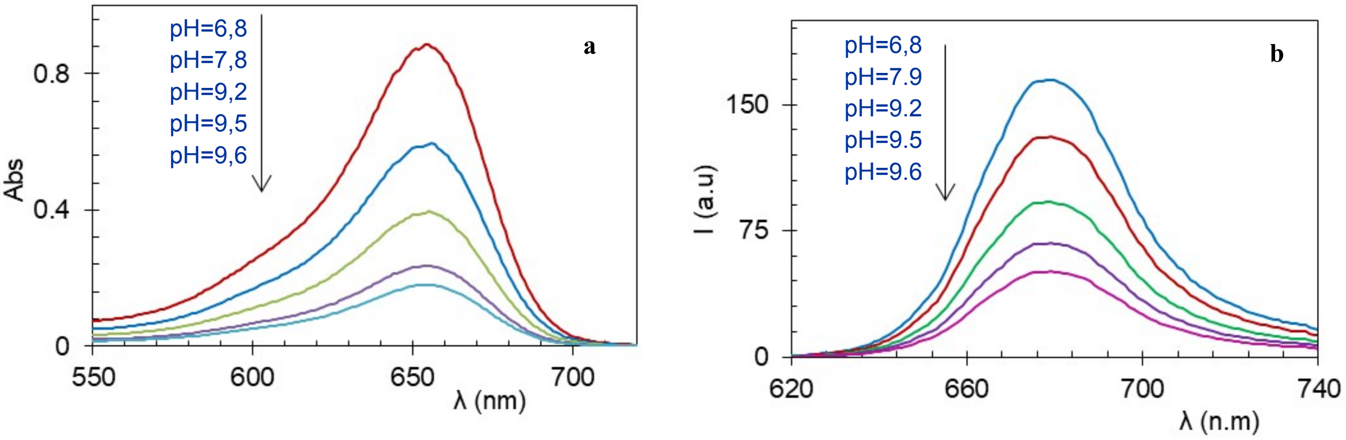

Figure S11. pH influence on azaBODIPY I: a) absorption spectrum; b) emission spectrum.

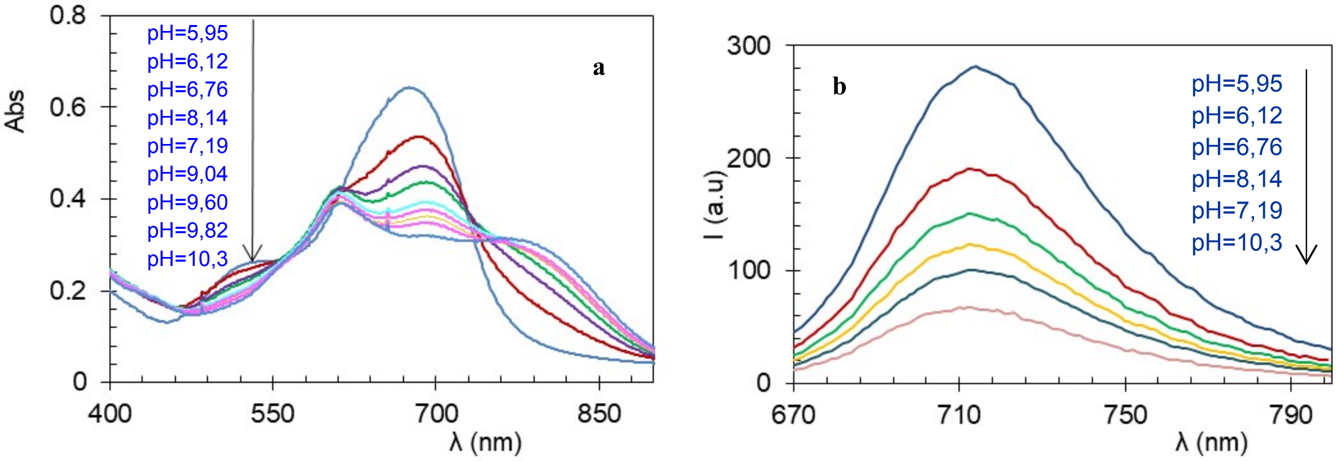

Figure S12. pH influence on azaBODIPY II: a) absorption spectrum; b) emission spectrum.

7. Optimization different components of sensing membranes

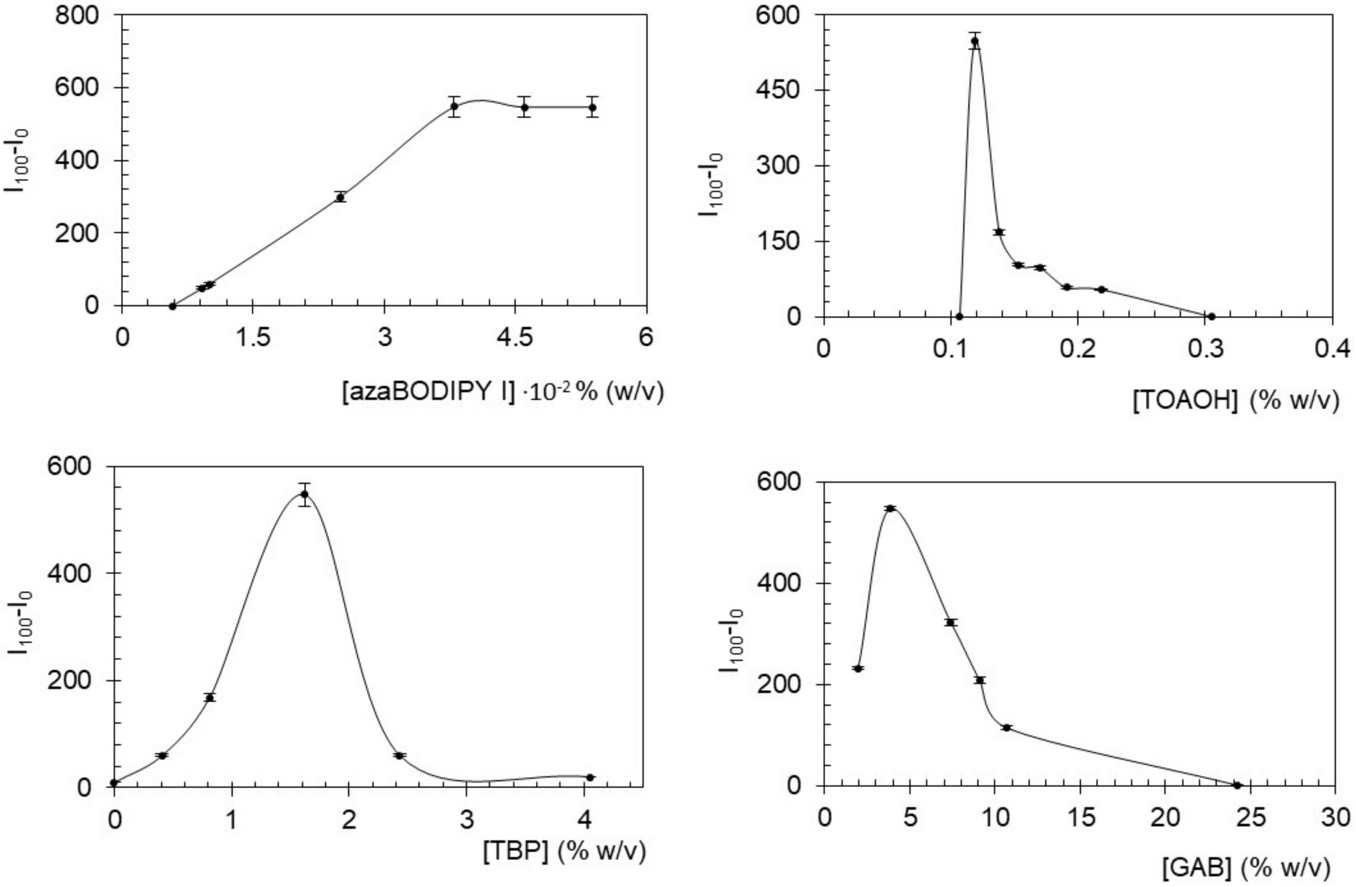

Figure S13. Optimizarion of concentration of components in sensing membrana using azaBODIPY I: a) concentration of azaBODIPY I; b) concentration of TOAOH; c) concentration of TBP and d) concentration of GAB.

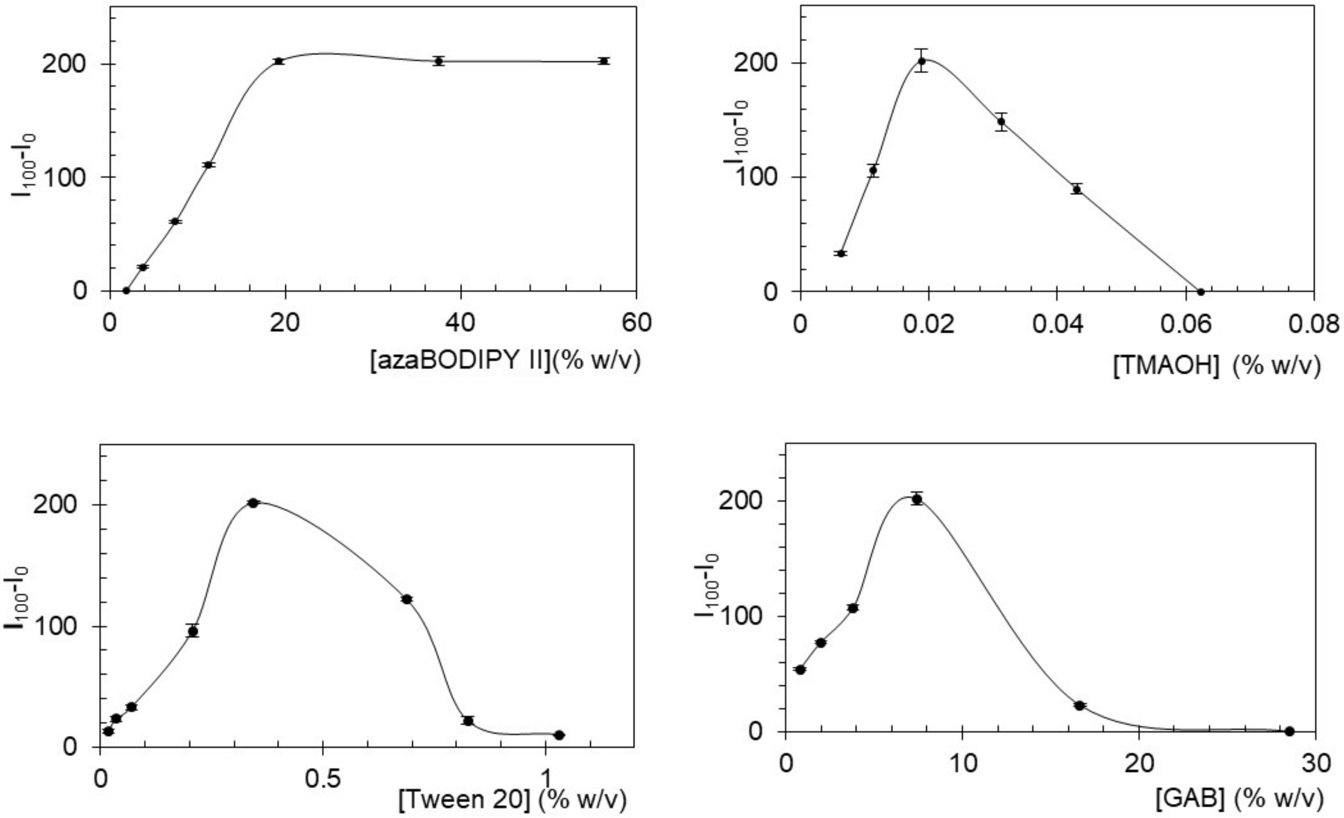

Figure S14. Optimizarion of concentration of components in sensing membrana using azaBODIPY II: a) concentration of azaBODIPY II; b) concentration of TMAOH; c) concentration of Tween 20 and d) concentration of GAB.

8. Supplementary Information References

1. S.M. Borisov, K. Gatterer, B. Bitschnau, I. Klimant, J.Phys.Chem.C, 2010, **114**, 9118.

2. W. Freyer, S. Mueller, K. Teuchner. Jour. Photochem. Photobio. A, 2004, **163,** 231.